Development and Evaluation of Kelakai Leaf Extract–Mediated Silver Nanoparticle Hydrogel for enhanced Antibacterial and Antibiofilm Performance

Lutfi Chabib
Islamic University of Indonesia
Farida Hayati
Islamic University of Indonesia
Viviane Annisa
Islamic University of Indonesia
Betty Ekawati Suryaningsih
Islamic University of Indonesia
Sri Sudewi
ssudewi@gmail.com

Sam Ratulangi University
M. Rifqi Fadillah Muslim
Islamic University of Indonesia

Research Article

Keywords: Silver nanoparticle, hydrogel, Stenochlaena palustris, antibacterial, antibiofilm

Posted Date: May 9th, 2026

DOI: https://doi.org/10.21203/rs.3.rs-9239136/v1

Additional Declarations: No competing interests reported.

Abstract

Purpose

Antibiotic resistance necessitates the development of alternative therapeutic agents, particularly those targeting biofilm formation. This study investigated the biosynthesis of silver nanoparticles (AgNPs) using *Stenochlaena palustris* (Kelakai) leaf extract and their formulation into a carbopol-based hydrogel system.

Method

Phytochemical identification of Kelakai (*Stenochlaena palustris*) leaf extract was conducted using thin-layer chromatography (TLC) with specific reagents to detect secondary metabolites such as flavonoids, phenols, tannins, steroids, terpenoids, saponins, and alkaloids. Silver nanoparticles (AgNPs) were biosynthesized by reacting the extract with 1 mM $AgNO_3$, and nanoparticle formation was indicated by a gradual color change of the solution over 24 hours. Particle size, polydispersity index, and surface charge were conducted using particle size analyzer and zeta potential. Morphological characterization using scanning electron microscopy (SEM) and transmission electron microscopy (TEM).The biosynthesized AgNPs were incorporated into a Carbopol 940 hydrogel and evaluated for stability, antibacterial activity against *Staphylococcus aureus* and *Escherichia coli*, and antibiofilm activity during both the attachment prevention and mature biofilm disruption stages.

Result

The extract served as a bioreducing agent to produce AgNPs, which were characterized as spherical structures with an average size of 101.1 nm. The synthesized nanoparticles were incorporated into hydrogels at varying concentrations and evaluated for physical stability, viscosity, spreadability, and adhesiveness. All formulations exhibited excellent physical stability following six freeze–thaw cycles. In antibacterial evaluations against *Staphylococcus aureus* and *Escherichia coli* using the disk diffusion method, the AgNP hydrogels produced significantly larger inhibition zones than their extract, with the highest concentration formulation exhibiting the most potent activity. Furthermore, antibiofilm assays demonstrated that the hydrogels significantly inhibited both the attachment and destruction phases of biofilm development compared to controls.

Conclusion

These findings suggest that AgNP-loaded hydrogels containing *Stenochlaena palustris* extract significantly enhance antimicrobial efficacy, with promising potential as topical formulations for managing bacterial infections and biofilm-associated conditions.

INTRODUCTION

Antibiotic resistance has been recognized as a significant public health threat by the World Health Organization (WHO), with antibiotic-resistant infections ranking as the third leading cause of death after cardiovascular and endocrine diseases. An estimated 1.27 million deaths were caused by antibiotic resistance in 2019 [1], with this figure projected to increase to 10 million per year by 2050, far exceeding deaths from cancer [2]. One of the causes of antibiotic resistance is biofilm, a structured community of microorganisms that produce extracellular polymeric substances (EPS), attach to the surfaces of living or non-living objects, and exhibit variations in growth and gene expression compared to their planktonic form [3]. Biofilms that produce EPS increase resistance to antibiotics and other external threats to the host [4]. With increasing resistance of bacteria and biofilms to antibacterial agents, other alternatives are needed to overcome this, one is the use of plants with potential antibacterial and antibiofilm activity.

Stenochlaena palustris (Burm.f) Bedd., commonly known as Kelakai, is a climbing fern in the family Blechnaceae and has long been used as a traditional medicinal plant by communities in Kalimantan. Although the specific bioactive marker compounds responsible for its antibacterial and antibiofilm effects have not been clearly identified, previous study reported that Stenopalustroside A–E, isolated from *S. palustris*, exhibited notable inhibitory activity against Gram-positive bacteria [5]. Despite several reports suggesting that Kelakai extracts possess antibacterial properties, other studies have shown only minimal or even negligible antibacterial activity [6][7]. These limitations highlight the challenges of using plant-based materials, particularly in crude extracts. Many plant extracts are poorly soluble or completely insoluble, resulting in low bioavailability, the need for repeated administration at high doses, and overall poor therapeutic performance [8]. One method to minimize this is by utilizing nanoparticles. For example, silver nanoparticles (AgNPs) are known to enhance antibacterial activity significantly [9].

Based on previous research, AgNPs exhibit good antimicrobial activity against various pathogens, including bacteria and fungi [10]. Green synthesis, or biosynthesis, of AgNPs is gaining increasing attention due to its simple, safe, and biocompatible nature [11]. Consequently, green-synthesized AgNPs offer advantages such as high stability, non-toxicity, low cost, and rapid production [12]. In addition, hydrogels have received considerable attention for their potential to enhance solubility, bioavailability, pharmacological activity, stability, and sustained delivery [13]

This study aims to formulate and evaluate a silver nanoparticle hydrogel loaded with Kelakai (*Stenochlaena palustris*) leaf extract, focusing on its physicochemical characteristics, antibacterial performance, and antibiofilm activity. The research seeks to determine its potential as an alternative therapeutic candidate against *Staphylococcus aureus* and *Escherichia coli*.

MATERIALS AND METHODS

Materials

In this study, the bacterial standards used were *Staphylococcus aureus* ATCC 25923 and *Escherichia coli* ATCC 25922, obtained and standardized from the Microbiology Laboratory at the Islamic University of Indonesia. Young brown Kelakai leaves are obtained from Muara Jawa District, Kutai Kartanegara Regency, East Kalimantan Province, Indonesia. The plant materials utilized in this investigation, specifically the wild-harvested *Stenochlaena palustris* (Burm.) Bedd. leaves, were collected in full compliance with relevant institutional and national botanical guidelines. Given that this fern is widely abundant and not classified under any protected or endangered status, specific statutory conservation permits were not required. Nonetheless, all sampling procedures were conducted ethically and with appropriate local consensus. To verify the botanical origin, the specimens were formally authenticated by taxonomist Ichsan Luqmana Indra Putra, S.Si., M.Sc.. A representative record and voucher details have been permanently deposited at the Biology Laboratory, Faculty of Applied Science and Technology, Universitas Ahmad Dahlan, Indonesia, under the official determination reference number 589/Lab.Bio/B/XI/2025. Ethanol 96% (Merck, Darmstadt, Germany), Carbopol® 940, and silver nitrate ($AgNO_3$) (Sigma Aldrich, St. Louis, USA) were purchased from CV. Sentra Teknosains (Yogyakarta, Indonesia). All other chemicals were of analytical grade.

Kelakai collection

Fresh leaves of *Stenochlaena palustris* (locally known as Kelakai) utilized in this study were harvested directly from their natural wild habitat. The sampling was conducted in Handil 2 Village, Muara Jawa Ulu, Muara Jawa Subdistrict, Kutai Kartanegara Regency, East Kalimantan Province, Indonesia. To ensure strict methodological traceability, the precise geographical coordinates of the collection site were recorded as 0°49'22.6"S, 117°14'43.1"E (-0.822935, 117.245312). Before collecting plant samples, representatives of the local community and landowners gave their informed agreement or authorization.

Kelakai leaf extract preparation

We began sample preparation by thoroughly washing young (brown) Kelakai leaves with water and then air-drying them. Once dry, we ground the leaves into a powder. In the extraction stage, we dissolved the leaf powder in 96% ethanol at a 1:10 ratio and processed it using an ultrasonic homogenizer (GT Sonic Ultrasonic 3L, Meizhou, China) at 30°C for 30 minutes.

Next, we filtered the sonication results using filter paper and re-extracted the residue using the same method. We then evaporated the filtrate using a rotary evaporator (Heidolph® Hei-Vap, Schwabach, Germany) until it thickened. We continued the evaporation process in a water bath to obtain a pure, thick extract. Finally, we stored the extract in a glass container at -2°C until ready for use.

Phytochemical identification

We conducted qualitative compound identification using Thin Layer Chromatography (TLC), adapting the protocol from Ramadhan *et al.* with minor modifications [14]. This screening targeted alkaloids, phenols, flavonoids, tannins, saponins, and steroids.

For the chromatographic system, we employed silica gel GF254 plates as the stationary phase and a solvent mixture of n-hexane and acetone (4:1) as the mobile phase. Prior to sample application, we pre-eluted the plates in a chamber saturated with 10 mL of methanol to prevent tailing, followed by activating them in an oven at 105°C for 1 minute. We prepared the test solution by dissolving Kelakai leaf extract in methanol (10 mg/mL) and applied a single spot onto the plate using a capillary tube.

AgNPs preparation

We synthesized AgNPs by adapting a previously reported method with minor modifications [15]. We first prepared the reducing agent by dissolving Kelakai leaf extract in deionized water (5%) under magnetic stirring. To initiate the reaction, we mixed 10 mL of the extract solution with 90 mL of 1 mM $AgNO_3$ and heated the mixture at 60°C for 2 hours with continuous stirring. We continued to monitor the reaction until we observed a color change to brownish-yellow after 24 hours.

Evaluation of biosynthesized AgNPs using Kelakai leaf extract

Evaluations including particle size, polydispersity index value, and zeta potential, were carried out using a Particle Size Analyzer (Horiba SZ-100, Kyoto, Japan). Morphological observations were carried out using a Scanning Electron Microscope (SEM) (Phenom Desktop ProXL, Thermo Fischer, Waltham, MA, USA) and a Transmission Electron Microscope (TEM) (Thermo Fischer, Waltham, MA, USA). SEM testing is the observation of a sample's surface structure using an electron beam to scan and produce electron images [16]. TEM testing is the observation of a sample's internal structure by passing an electron beam through it to produce an image [17].

Formulation of biosynthesized AgNPs hydrogel

We developed the hydrogel formulation based on prior studies, incorporating minor modifications [18]. We prepared the gel base by dispersing Carbopol 940 in deionized water under vigorous stirring using a homogenizer (IKA Ultra-Turrax® T-50, Staufen, Germany). Subsequently, we gradually added glycerin as a humectant. To adjust the pH and preserve the mixture, we introduced TEA and methyl paraben, stirring continuously until the gel became homogeneous. Finally, we slowly incorporated the AgNPs into the Kelakai leaf extract mixture until we achieved a uniform consistency. The detailed formulation composition is listed in Table 1.

Table 1
Design formula for hydrogel loaded with AgNPs using Kelakai leaf extract

Materials	F1	F2	F3
AgNPs using Kelakai leaf extract	1%	1,5%	2%
Carbopol 940	0,5%	0,5%	0,5%
Glycerin	5%	5%	5%
Triethanolamine	1%	1%	1%
Methyl paraben	0,15%	0,15%	0,15%
Deionized water	Ad to 100%	Ad to 100%	Ad to 100%
Notes: Ad to 100% indicates the formula was adjusted to a total of 100% using deionized water			

Evaluation of biosynthesized AgNPs hydrogel

Stability test

The stability test was carried out using the freeze-thaw stability test method for six cycles at a temperature of 4°C for 24 hours and then at a temperature of 40°C for 24 hours [19].

Organoleptic test

Organoleptic testing involves observing the formulation's consistency, color, and odor. Homogeneity testing is performed by applying 1 g of the preparation to two glass slides. The preparation must be homogeneous, showing no coarse grains.

Viscosity test

Viscosity was measured using a Brookfield viscometer (DV-I Prime, Middleboro, MA, USA) using Spindle 64 at a speed of 50 rpm.

Spreadability test

The preparation is weighed to 0.5 g, then placed between two glass slides. A load of 50 g is added, left for one minute, and the diameter of the spread preparation is measured.

Adhesive strenght test

A 0.5 g sample is weighed and placed on a slide, then weighed down with another slide, and then given a 1 Kg load for five minutes. The slide is then mounted on the adhesive strength tester, and the time it takes for the two slides to detach is recorded.

Antibacterial activity test

The disk diffusion method was used for antibacterial testing against *S. aureus* and *E. coli* bacteria. *S. aureus* and *E. coli* bacterial cultures were dissolved in 0.9% NaCl to obtain the same turbidity level as the 0.5 McFarland standard of approximately 1.0×10^8 CFU/mL. The bacterial suspension was then spread on the surface of the MHA medium using a sterile cotton swab. Seven paper disks were then placed on the medium consisting of 10 mg/mL chloramphenicol as a positive control, distilled water as a negative control, 10 mg/mL Kelakai leaf extract, 10 mg/mL $AgNO_3$ solution, and 10 mg/mL of each biosynthesized AgNPs hydrogel formula (F1, F2, F3). The bacterial cultures were incubated for 24 hours at 37°C. Each treatment was carried out three times in a replicated design.

Anti-biofilm assay

Biofilm inhibition was performed using a modified method described by Olawuwo *et al* [20]. The test was conducted in two phases of biofilm development: prevention of biofilm attachment (P1) and destruction of biofilm formation after 24 hours (P2). Biofilm testing was carried out using a positive control sample group (culture + MHB + chloramphenicol), a negative control (culture + MHB), a sample control [culture + MHB + sample (Kelakai leaf extract, $AgNO_3$ solution, and each biosynthesized AgNPs hydrogel formula)], and a media control (MHB only) at a final concentration of 10 mg/mL. In the P1 test, a standardized bacterial culture (1.0×10^6 CFU/mL) in Mueller-Hinton Broth (MHB) was added to a 96-well microplate to a final volume of 100 µL, followed by the addition of 100 µL of each sample, and incubated for 24 hours at 37°C. For P2, 100 µL of standardized bacterial culture was pre-incubated for 24 hours to establish biofilm growth, then each sample was added.

After incubation, the well contents were gently removed, the plate was washed three times with sterile deionized water, and then dried at room temperature for 15 minutes. Then, 200 µL of 0.1% crystal violet was added to stain adherent cells, which were then dried for 30 minutes at room temperature. Excess color was rinsed five times with sterile deionized water. Then, 200 µL of 96% ethanol was added to each well to remove the color. The absorbance of the plate was measured at 590 nm using an ELISA reader (Thermo Fisher). The mean absorbance (OD_{590nm}) of the samples was determined, and the results were expressed as percentage inhibition using the following equation [21].

$$\text{Percentage (\%) inhibition} = \frac{ODNegative\ control - ODSample}{ODNegative\ control} \times 100\%$$

RESULTS

The percentage of Kelakai leaf extraction

Processing 500 g of dried powder with 5 L of 96% ethanol, we obtained 72.36 g of viscous extract. This quantity corresponds to a 14.47% yield relative to the starting material. Table 2 summarizes the detailed extraction data.

Table 2
The result of percentage yield of Kelakai leaf extraction

Simplicia weight (g)	Extract weight (g)	Yield percentage (%)
500	72.36	14.47

Phytochemical identification

We confirmed the presence of diverse secondary metabolites in the Kelakai leaf extract through TLC visualization. Upon spraying with specific reagents, we observed distinct spots indicating the presence of flavonoids ($AlCl_3$ 1%), as well as phenols and tannins, which both reacted positively to $FeCl_3$ 1% and Folin-Ciocalteu. Furthermore, the application of Liebermann-Burchard reagent identified both steroids and terpenoids, while vanillin-sulfuric acid detected saponins. Regarding alkaloids, we noted a positive reaction with 5% sulfuric acid, although Dragendorff's reagent yielded a negative result. These findings demonstrate that the extract possesses a rich phytochemical profile essential for the bioreduction process in Table 3.

Table 3
Phytochemical identification result through TLC

Tests	Reagents	Result
Alkaloid	Sulfuric acid 5%	+
	Dragendorff	-
Flavonoid	$AlCl_3$ 1%	+
Phenol	$FeCl_3$ 1%	+
	Folin-Ciocalteu	+
Tannin	$FeCl_3$ 1%	+
	Folin-Ciocalteu	+
Steroid	Liebermann-Burchard	+
Terpenoid	Liebermann-Burchard	+
Saponin	Vanillin-sulfuric acid	+
Note:		
+ : spots formed after spraying with reagents		
- : no spots formed after spraying with reagents		

Biosynthesized AgNPs using Kelakai leaf extract

We monitored the biosynthesis process through direct visual inspection, noting that increased turbidity and color shifts indicate AgNPs formation [9]. Upon reacting the $AgNO_3$ precursor with Kelakai leaf extract, we observed the initially clear, pale yellow solution gradually deepen in intensity over 24 hours, as Fig. 1 illustrates.

Particle size analysis (PSA)

The biosynthesized AgNPs produced from Kelakai leaf extract using one mM AgNO3 as the precursor had an average diameter of 101.1 nm. The polydispersity index was 0.553, and the zeta potential was −27.4 mV, as shown in Table 4. Nanoparticles containing metal ions, such as Ag, exhibit a broader absorption spectrum, leading to larger particle sizes and greater polydispersity [22].

Table 4
The particle size analysis of biosynthesized AgNPs using Kelakai leaf extract

Particle size (nm)	Polidispersity index	Zeta potential (mV)
101,1 ± 1,05	0,553 ± 0,001	-27,4 ± 0,1

Scanning electron microscope (SEM) and Transmission electron microscope (TEM)

SEM observations showed that the nanoparticles were spherical or round individually, while some aggregates were irregularly shaped. Moieties present in the Kelakai extract induced spherical shapes in the nanoparticles, while the aggregates observed may be due to secondary metabolites in the extract [23]. TEM observations revealed a spherical nanoparticle structure with a size range of 20–100 nm. SEM and TEM images are shown in Fig. 2.

Evaluation of biosynthesized AgNPs hydrogel

We selected Carbopol 940 as the gelling agent due to its favorable physicochemical profile. Its non-toxic nature and capability to gel at room temperature allow for processing without heat, thereby preserving the stability of temperature-sensitive herbal compounds [24]. Figure 3 illustrates the macroscopic appearance of the resulting biosynthesized AgNPs hydrogel.

Regarding stability, the formulations underwent six freeze-thaw cycles without phase separation or degradation. Organoleptic evaluation characterized all three formulations as transparent green, semi-solid gels with a distinctive odor and viscous consistency. Additionally, homogeneity testing confirmed the absence of coarse particles throughout the cycles. Figure 4 details the viscosity, spreadability, and adhesiveness metrics, which demonstrated no significant fluctuations across the formulations during the testing period.

Antibacterial activity using disk diffusion method

The antibacterial activity was evaluated against two representative pathogenic bacteria, *S. aureus* (Gram-positive) and *E. coli* (Gram-negative), by measuring the diameter of the inhibition zones formed in Fig. 5. In general, all hydrogel formulations containing AgNPs (F1–F3) showed a significant increase in antibacterial activity compared to extract control (EC).

In the test against *S. aureus* (Fig. 5A), the positive control (PC) produced the largest inhibition zone, validating the test bacteria's sensitivity. The extract control (EC) showed only weak to moderate inhibitory activity. However, when formulated into an AgNPs hydrogel system, there was a significant increase in activity. Formulation F3 showed the largest inhibition zone diameter, reaching approximately 16 mm. Statistical analysis confirmed that F3 had the highest significant difference ($p < 0.0001$) compared to EC, followed by F2 ($p < 0.001$) and F1 ($p < 0.05$). This trend indicates a dose-dependent activity, where increasing AgNP concentration in the hydrogel is directly proportional to the bacterial inhibition capacity.

A similar pattern was observed in the test against *E. coli* (Fig. 5B), albeit with a slightly lower inhibitory response compared to *S. aureus*. Formulation F3 again demonstrated superior performance, with an inhibition zone of approximately 11 mm, far exceeding the EC activity of approximately 4 mm. Although Gram-negative bacteria have a complex lipopolysaccharide outer membrane defence, formulation F3 still provided a highly significant inhibitory effect ($p < 0.0001$) compared to the extract control.

Anti-biofilm activity

The anti-biofilm potential of AgNPs hydrogels was evaluated at two critical stages of biofilm development: the attachment prevention phase (P1) and the mature biofilm synchronisation phase (P2), which involves the disintegration of the formed biofilm, against *S. aureus* and *E. coli* in Fig. 6.

The hydrogel formulations (F1–F3) demonstrated significantly greater anti-biofilm efficacy than the extract control (EC). Testing against *S. aureus* (Fig. 6A) showed that the formulations ability to prevent initial biofilm formation (P1) was more effective than their ability to degrade the 24-hour-old biofilm matrix (P2). Formulation F3 recorded the highest inhibition percentage, exceeding 60% in the P1 phase, while maintaining vigorous activity in the P2 phase. Statistical analysis showed a very high level of significance (****: $p < 0.0001$) for F3 compared with the extract control group (EC), indicating that the nanoparticle system in the hydrogel significantly contributes to disrupting the bacterial biofilm life cycle.

Consistent results were also found in the test against *E. coli* (Fig. 6B). Although Gram-negative bacteria often exhibit higher resistance due to the complexity of their extracellular matrix, the AgNPs hydrogel formulation still provided significant inhibition. Formula F3 again emerged as the superior agent, with biofilm destruction (P2) remaining significant (****: $p < 0.001$) compared to EC. The drastic decrease in antibiofilm activity in the extract control group (EC) upon entering the P2 phase in contrast to the stable

levels in groups F1-F3 confirms that the presence of AgNPs allows for better penetration through the protective biofilm layer.

DISCUSSION

The biosynthesis of silver nanoparticles (AgNPs) via plant extracts presents a sustainable, eco-friendly alternative to conventional chemical routes. In this mechanism, endogenous phytochemicals such as polyphenols, flavonoids, and terpenoids function dualistically, they reduce Ag^{+} ions to metallic Ag^{0} nanoparticles and simultaneously stabilize the resulting colloids. Extensive literature validates that this green approach generates stable AgNPs possessing diverse biological functionalities, notably antibacterial and antioxidant properties [25].

We attribute the successful biosynthesis of AgNPs to the diverse secondary metabolites identified in the Kelakai leaf extract, particularly phenols, flavonoids, and tannins. We posit that these compounds function as dual-action agents, reducing Ag^{+} ions and stabilizing the resulting nanoparticles. Specifically, the hydroxyl (-OH) groups abundant in flavonoid and phenolic structures facilitate the reduction of Ag^{+} to elemental Ag^{0} by donating electrons/hydrogen, a mechanism corroborated by the distinct color change we observed during synthesis [26].

Regarding the alkaloid test, the conflicting results, positive with sulfuric acid but negative with Dragendorff suggest that alkaloids likely act as minor constituents or require more specific extraction methods, thus playing a subordinate role compared to the dominant polyphenols. Furthermore, we hypothesize that the detected saponins and macromolecules (steroids/terpenoids) contribute to steric stabilization, coating the nanoparticles and preventing agglomeration [27][28]. Consequently, our data confirms that Kelakai extract possesses the ideal chemical profile to serve as an effective, eco-friendly bioreductor.

In this study, the color transition from pale yellow to brown within 24 hours strongly supports the formation of AgNPs, consistent with typical green-synthesis pathways. The phytochemical profile of Kelakai, particularly the presence of stenopalustrosides and polyphenolic constituents, likely played a crucial role in nanoparticle formation. These compounds may have provided abundant hydroxyl groups, facilitating electron donation to silver ions and promoting nucleation and particle growth. Similar mechanisms have been reported in fern-derived extracts, which contain phenolic-rich matrices capable of stabilizing AgNPs [29]. Although the use of Kelakai in AgNPs biosynthesis has not been widely studied, the general principles of other plant biosynthesis are relevant. The use of Kelakai to reduce Ag^{+} ions shows great potential, given its efficient bioreductant properties. Mechanistically, the phenolic compounds in Kelakai play a role in reducing Ag^{+} to AgNPs and also function as encapsulating agents, preventing agglomeration and increasing colloidal stability [30].

The biological performance of AgNPs is strongly influenced by particle size, morphology, and surface characteristics. In Fig. 2, TEM analysis revealed predominantly spherical nanoparticles measuring 20–100 nm, while PSA indicated an overall diameter of 101.1 nm. Previous studies show that AgNPs below

100 nm exhibit enhanced antibacterial activity due to their ability to penetrate bacterial membranes, generate reactive oxygen species (ROS), and disrupt intracellular components [31]. Spherical morphology is often associated with a higher surface-to-volume ratio, which facilitates greater ion release and contributes significantly to antimicrobial activity [32]. Particle aggregation observed in SEM is common in plant-mediated synthesis and may partially reduce surface area. However, the remaining fraction of well-dispersed nanoparticles appears sufficient to support vigorous antibacterial and antibiofilm activity [33]. Thus, the nanoscale dimensions and spherical morphology of the Kelakai-derived AgNPs likely contributed to their superior antimicrobial performance compared with crude extracts. These physicochemical features enable efficient interaction with bacterial surfaces and deeper penetration into biofilm matrices, explaining the significant enhancement in activity observed across formulations.

Incorporating biosynthesized AgNPs into a hydrogel matrix provides several advantages that enhance both stability and therapeutic performance. Hydrogels offer a three-dimensional polymeric network that retains high water content, thereby improving spreadability, skin adhesion, and patient comfort. Carbopol-based hydrogels, such as those used in this study, are known for their excellent rheological properties, biocompatibility, and ability to sustain the release of active agents [34]. Embedding AgNPs in a hydrogel creates a controlled microenvironment that stabilizes nanoparticles by reducing aggregation and slowing oxidation processes. Previous reports demonstrate that hydrogel-encapsulated AgNPs exhibit longer shelf stability and more consistent antimicrobial performance than their free nanoparticle counterparts [35]. The freeze-thaw results in this study further confirm that the hydrogel matrix maintains structural integrity across temperature fluctuations, supporting its robustness as a delivery platform.

The moisturizing properties of hydrogels also enhance drug permeation and retention at the application site. This is particularly beneficial against biofilms, which often form in chronic wounds or moist environments [36]. Hydrogels facilitate prolonged contact between AgNPs and bacterial communities, allowing sustained silver ion release, deeper penetration into biofilm layers, and disruption of EPS structures [37]. Combining Kelakai extract with AgNPs in a hydrogel leverages synergistic effects between plant-derived phytochemicals and nanoparticulate silver. The extract may enhance membrane disruption or inhibit early biofilm adhesion, complementing the ROS-mediated antibacterial effect of AgNPs.

The antibacterial test in Fig. 5 and **Figure S1** demonstrated apparent differences in inhibition zone diameters among the tested samples against *S. aureus* and *E. coli*. The results showed that incorporating AgNPs into the hydrogel matrix significantly increased bactericidal effectiveness compared to the pure extract. This increase in the inhibition zone is directly related to the physicochemical characteristics of AgNPs. The nanoscale particle size provides a massive contact surface area, facilitating the continuous release of silver ions from the hydrogel matrix to the bacterial cell wall [38].

Specifically, antibacterial activity against *S. aureus* (Fig. 5A) appears to be greater than against *E. coli* (Fig. 5B). In F3, the inhibition zone of *S. aureus* reached around 16 mm, while *E. coli* was around 11 mm (**Figure S1A-D**). This difference occurs because *E. coli* is a Gram-negative bacterium with a complex lipopolysaccharide outer membrane layer, which functions as an additional barrier, making it more difficult for antibacterial agents to penetrate than in *S. aureus* (Gram-positive), which has only a simple peptidoglycan layer [39]. The primary mechanism of bacterial inhibition is through the interaction of silver ions with thiol groups (-SH) on bacterial membrane proteins, which disrupts cell wall integrity and causes cytoplasmic leakage. In addition, AgNPs induce the formation of Reactive Oxygen Species (ROS) within cells that disrupt DNA replication and cellular respiration [40].

The results of the anti-biofilm hydrogel testing based on biosynthesized AgNPs showed a dose-dependent activity pattern, where formulation F3 (the highest concentration of AgNPs) consistently showed the most superior inhibition compared to the control extract (EC) in both critical phases of biofilm development: the initial adhesion phase (P1) and the maturation phase (P2). In the P1 (Prevention of Attachment) phase, the high inhibition percentage in F3 (Fig. 6A) can be attributed to the ability of AgNPs to modify the physicochemical properties of the bacterial cell surface. Silver nanoparticles are known to neutralize electrostatic charges on the cell wall and alter the hydrophobicity of the bacterial surface, thereby reducing the affinity of bacterial attachment to the substrate. This mechanism is crucial because irreversible adhesion is the initiating step in biofilm formation by blocking it, bacterial colonization can be prevented early [41].

Substantial challenge arises in the P2 phase (Destruction of Pre-formed Biofilm), where a dense Extracellular Polymeric Substance (EPS) matrix shields the bacterial colonies. The sharp decline in activity observed in the extract control (EC) suggests that the macromolecular compounds in the extract were unable to penetrate this barrier. In contrast, the AgNPs formulations (F1–F3) retained significant efficacy, underscoring the critical advantage of their nanometric size (Fig. 6A). This structural property facilitates deep penetration into biofilm water channels, enabling sustained release of silver ions to disrupt the matrix architecture and compromise the DNA of embedded persister bacteria [42].

Notably, the AgNPs hydrogels exhibited robust activity against Gram-negative *E. coli* (Fig. 6B), effectively overcoming the challenge posed by its outer membrane lipopolysaccharide (LPS). This observation aligns with contemporary findings, in which AgNPs accumulate on the outer membrane, inducing 'pit' formation that compromises structural integrity and leads to cytoplasmic leakage [43]. In parallel, the superior efficacy against Gram-positive *S. aureus* is likely attributable to the dense peptidoglycan layer, which acts as a reservoir, entrapping the nanoparticles and thereby facilitating sustained, localised release of oxidative ions (Fig. 6A) [44].

CONCLUSION

This study has successfully demonstrated the effectiveness of *Stenochlaena palustris* (Kelakai) leaf extract as a natural bioreductant in the green synthesis of silver nanoparticles (AgNPs).

Physicochemical analysis confirmed the formation of spherical nanoparticles with an average size of 101.1 nm that have good colloidal stability. When formulated into a Carbopol 940-based hydrogel delivery system, the resulting preparation not only exhibited ideal physical characteristics and was stable during temperature cycling, but also provided a significant increase in biological activity compared to the pure extract. A crucial finding of this study was a dose-dependent correlation, with Formula 3 (the highest concentration) showing the most substantial bactericidal potential against Staphylococcus aureus and Escherichia coli, as well as superior ability to inhibit initial biofilm formation and degrade mature biofilm matrices. Thus, this Kelakai extract-based AgNPs hydrogel offers promising prospects as a new topical preparation candidate for the treatment of bacterial infections and biofilm-based resistance.

Declarations

Ethics approval and consent to participate

Not applicable.

Consent for publication

Not applicable.

Conflict of Interest

The authors declare no conflicts of interest.

Author Contribution

Conceptualization, writing-original draft preparation, and data curation, funding acquisition, L.C.; methodology, and data curation, F.H.; data curation, investigation, V.A; methodology, software, investigation, B.E.S.; visualization, formal analysis, M.R.F.M.; resources, supervision, and validation, S.S. All authors have read and agreed to the published version of the manuscript.

Acknowledgement

The author(s) would like to extend their appreciation to the Ministry of Education, Culture, Research, and Technology of Indonesia, Grant. No. 031/DirDPPM/70/DPPM/PFR-KEMDIKTISAINTEK/VI/2025 and Hibah Penelitian Unggulan, Directorate of Research and Community Service, Universitas Islam Indonesia, Grant No. 013/DPPM//70/Pen.Unggulan/IV/2025, Department of Pharmacy, Faculty of Mathematics and Natural Sciences, Universitas Islam Indonesia, Yogyakarta, Indonesia. for the support in this research.

Data Availability

The datasets supporting the conclusions of this article are included within the manuscript and its supplementary files. Additional raw data can be provided by the corresponding author upon reasonable request.

References

1. C. J. L. Murray *et al.*, “Global burden of bacterial antimicrobial resistance in 2019: a systematic analysis,” *The Lancet*, vol. 399, no. 10325, pp. 629–655, Feb. 2022, doi: 10.1016/S0140-6736(21)02724-0.
2. O. M. Ghimpețeanu *et al.*, “Antibiotic Use in Livestock and Residues in Food—A Public Health Threat: A Review,” *Foods*, vol. 11, no. 10, p. 1430, May 2022, doi: 10.3390/foods11101430.
3. M. A. Rather *et al.*, “Microbial biofilm: A matter of grave concern for human health and food industry,” *J Basic Microbiol*, vol. 61, no. 5, pp. 380–395, May 2021, doi: 10.1002/jobm.202000678.
4. R. Grande, V. Puca, and R. Muraro, “Antibiotic resistance and bacterial biofilm,” *Expert Opinion on Therapeutic Patents*, vol. 30, no. 12, pp. 897–900, Dec. 2020, doi: 10.1080/13543776.2020.1830060.
5. H. Liu, J. Orjala, O. Sticher, and T. Rali, “Acylated Flavonol Glycosides from Leaves of *Stenochlaena palustris*,” *J. Nat. Prod.*, vol. 62, no. 1, pp. 70–75, Jan. 1999, doi: 10.1021/np980179f.
6. R. Handayani and H. Rusmita, “Uji Daya Hambat Ekstrak Etanol Akar Kelakai (Stenochlaena palustris (Burm. F.) Bedd.) terhadap Bakteri Escherichia coli,” *J Surya Medika*, vol. 2, no. 2, pp. 13–26, Feb. 2017, doi: 10.33084/jsm.v2i2.356.
7. R. Hendra *et al.*, “Free Radical Scavenging, Anti-Infectious, and Toxicity Activities from Stenochlaena palustris (Burm.f.) Bedd. Extracts,” *Advances in Pharmacological and Pharmaceutical Sciences*, vol. 2022, pp. 1–8, Nov. 2022, doi: 10.1155/2022/5729217.
8. K. Kesarwani and R. Gupta, “Bioavailability enhancers of herbal origin: An overview,” *Asian Pacific Journal of Tropical Biomedicine*, vol. 3, no. 4, pp. 253–266, Apr. 2013, doi: 10.1016/S2221-1691(13)60060-X.
9. S. S. Bahry, A. Susilowati, and A. Pangastuti, “Characterization and antibacterial activity of biosynthesized silver nanoparticles using Stachytarpheta jamaicensis leaf extract as bioreduction,” *Indones. J. Biotechnol.*, vol. 30, no. 1, p. 1, Mar. 2025, doi: 10.22146/ijbiotech.88438.
10. N. Mujaddidi *et al.*, “Pharmacological properties of biogenically synthesized silver nanoparticles using endophyte Bacillus cereus extract of Berberis lyceum against oxidative stress and pathogenic multidrug-resistant bacteria,” *Saudi Journal of Biological Sciences*, vol. 28, no. 11, pp. 6432–6440, Nov. 2021, doi: 10.1016/j.sjbs.2021.07.009.
11. M. H. Bafghi, R. Nazari, M. Darroudi, M. Zargar, and H. Zarrinfar, “The effect of biosynthesized selenium nanoparticles on the expression of *CYP51A* and *HSP90* antifungal resistance genes in *Aspergillus fumigatus* and *Aspergillus flavus* ,” *Biotechnology Progress*, vol. 38, no. 1, p. e3206, Jan. 2022, doi: 10.1002/btpr.3206.

12. S. Marouzi, Z. Sabouri, and M. Darroudi, “Greener synthesis and medical applications of metal oxide nanoparticles,” *Ceramics International*, vol. 47, no. 14, pp. 19632–19650, Jul. 2021, doi: 10.1016/j.ceramint.2021.03.301.
13. I. Khan, K. Saeed, and I. Khan, “Nanoparticles: Properties, applications and toxicities,” *Arabian Journal of Chemistry*, vol. 12, no. 7, pp. 908–931, Nov. 2019, doi: 10.1016/j.arabjc.2017.05.011.
14. H. Ramadhan, D. P. Rezky, and E. F. Susiani, “Penetapan Kandungan Total Fenolik-Flavonoid pada Fraksi Etil Asetat Kulit Batang Kasturi (Mangifera casturi Kosterman),” *JFIKI*, vol. 8, no. 1, p. 58, Apr. 2021, doi: 10.20473/jfiki.v8i12021.58-67.
15. S. Ibrahim and A. Al-Niaame, “Formulation and evaluation of hydrogel incorporated with biosynthesis silver nanoparticles using aqueous extract of salvia officinalis l. Against s. Aureus isolated from wounds from some baghdad hospitals,” *Plant Archives*, pp. 449–456, Jan. 2020.
16. D. Garibo *et al.*, “Green synthesis of silver nanoparticles using Lysiloma acapulcensis exhibit high-antimicrobial activity,” *Sci Rep*, vol. 10, no. 1, p. 12805, Jul. 2020, doi: 10.1038/s41598-020-69606-7.
17. A. C. P. D. Santos, F. A. Dutra, R. Barin, W. L. D. Silva, and C. R. B. Rhoden, “An overview of the healing potential of silver nanoparticles in the treatment of diabetic wounds,” *CeN*, vol. 46, p. e86600, Oct. 2024, doi: 10.5902/2179460X86600.
18. N. N. Fajriyah *et al.*, “Topical nano hydrogel formulation of annona muricata extract enrich with zinc for improved therapy design and evaluation,” presented at the 3RD INTERNATIONAL CONFERENCE OF BIO-BASED ECONOMY FOR APPLICATION AND UTILITY, Padang, Indonesia, 2023, p. 020141. doi: 10.1063/5.0120738.
19. A. N. Zam Zam and M. Musdalifah, “Formulasi dan Evaluasi Kestabilan Fisik Krim Ekstrak Biji Lada Hitam (Piper nigrum L.) Menggunakan Variasi Emulgator,” *JSSCR*, vol. 4, no. 2, pp. 304–313, Apr. 2022, doi: 10.37311/jsscr.v4i2.14146.
20. O. S. Olawuwo, I. M. Famuyide, and L. J. McGaw, “Antibacterial and Antibiofilm Activity of Selected Medicinal Plant Leaf Extracts Against Pathogens Implicated in Poultry Diseases,” *Front. Vet. Sci.*, vol. 9, p. 820304, Mar. 2022, doi: 10.3389/fvets.2022.820304.
21. L. Chabib, H. Hamzah, W. Rahmah, S. F. Sammulia, E. Setyowati, and A. Nurfitrian, “Tracking of the Antibiofilm Activities of Lakum Leaf Extract (Causonis trifolia Linn.) Against Staphylococcus aureus,” *Pakistan J. of Biological Sciences*, vol. 26, no. 2, pp. 91–100, Jan. 2023, doi: 10.3923/pjbs.2023.91.100.
22. M. Ghebretatios, S. Schaly, and S. Prakash, “Nanoparticles in the Food Industry and Their Impact on Human Gut Microbiome and Diseases,” *IJMS*, vol. 22, no. 4, p. 1942, Feb. 2021, doi: 10.3390/ijms22041942.
23. N. Ahmad, S. N. A. Bukhari, M. A. Hussain, H. Ejaz, M. U. Munir, and M. W. Amjad, “Nanoparticles incorporated hydrogels for delivery of antimicrobial agents: developments and trends,” *RSC Adv.*, vol. 14, no. 19, pp. 13535–13564, 2024, doi: 10.1039/D4RA00631C.
24. F. I. Safitri, D. Nawangsari, and D. Febrina, “Overview: Application of Carbopol 940 in Gel:,” in *Proceedings of the International Conference on Health and Medical Sciences (AHMS 2020)*,

Yogyakarta, Indonesia: Atlantis Press, 2021. doi: 10.2991/ahsr.k.210127.018.

25. M. Fahim, A. Shahzaib, N. Nishat, A. Jahan, T. A. Bhat, and A. Inam, “Green synthesis of silver nanoparticles: A comprehensive review of methods, influencing factors, and applications,” *JCIS Open*, vol. 16, p. 100125, Dec. 2024, doi: 10.1016/j.jciso.2024.100125.
26. P. Bhati *et al.*, “Green synthesis of silver NPs using aqueous extract of Artemisia scoparia for hydrogenation of aromatic nitro compounds and their biological activity,” *Front. Microbiol.*, vol. 16, p. 1584066, Apr. 2025, doi: 10.3389/fmicb.2025.1584066.
27. B. Tessema, G. Gonfa, S. M. Hailegiorgis, S. V. Prabhu, and S. Manivannan, “Synthesis and characterization of silver nanoparticles using reducing agents of bitter leaf (Vernonia amygdalina) extract and tri-sodium citrate,” *Nano-Structures & Nano-Objects*, vol. 35, p. 100983, Jul. 2023, doi: 10.1016/j.nanoso.2023.100983.
28. O. Velgosova, S. Dolinská, H. Podolská, L. Mačák, and E. Čižmárová, “Impact of Plant Extract Phytochemicals on the Synthesis of Silver Nanoparticles,” *Materials*, vol. 17, no. 10, p. 2252, May 2024, doi: 10.3390/ma17102252.
29. P. Das, T. Dutta, S. Manna, S. Loganathan, and P. Basak, “Facile green synthesis of non-genotoxic, non-hemolytic organometallic silver nanoparticles using extract of crushed, wasted, and spent Humulus lupulus (hops): Characterization, anti-bacterial, and anti-cancer studies,” *Environmental Research*, vol. 204, p. 111962, Mar. 2022, doi: 10.1016/j.envres.2021.111962.
30. F. Arshad *et al.*, “Bioinspired and Green Synthesis of Silver Nanoparticles for Medical Applications: A Green Perspective,” *Appl Biochem Biotechnol*, vol. 196, no. 6, pp. 3636–3669, Jun. 2024, doi: 10.1007/s12010-023-04719-z.
31. V. A. Ershov and B. G. Ershov, “Effect of Silver Nanoparticle Size on Antibacterial Activity,” *Toxics*, vol. 12, no. 11, p. 801, Nov. 2024, doi: 10.3390/toxics12110801.
32. G. Carreño, S. Piñero, M. Delgado, Lady Quintero, J. Gutierrez, and S. Blanco, “Systematic control of silver nanoparticle size and shape for enhanced biocompatibility and antibacterial activity against *Staphylococcus aureus* and *Escherichia coli*,” *Oxford Open Materials Science*, vol. 5, no. 1, p. itaf016, Jan. 2025, doi: 10.1093/oxfmat/itaf016.
33. A. Y. Ali, A.-A. K. Alani, B. O. Ahmed, and L. L. Hamid, “Effect of biosynthesized silver nanoparticle size on antibacterial and anti-biofilm activity against pathogenic multi-drug resistant bacteria,” *OpenNano*, vol. 20, p. 100213, Nov. 2024, doi: 10.1016/j.onano.2024.100213.
34. M. Zintle *et al.*, “Antibacterial study of carbopol-mastic gum/silver nanoparticle-based topical gels with carvacrol/neem bark extract in vitro,” *J Wound Care*, vol. 32, no. Sup9a, p. clxxxi–clxxxix, Sep. 2023, doi: 10.12968/jowc.2023.32.Sup9a.clxxxi.
35. J. Yu *et al.*, “A Lignin Silver Nanoparticles/Polyvinyl Alcohol/Sodium Alginate Hybrid Hydrogel with Potent Mechanical Properties and Antibacterial Activity,” *Gels*, vol. 10, no. 4, p. 240, Apr. 2024, doi: 10.3390/gels10040240.
36. Y. Huangfu *et al.*, “Skin-Adaptable, Long-Lasting Moisture, and Temperature-Tolerant Hydrogel Dressings for Accelerating Burn Wound Healing without Secondary Damage,” *ACS Appl. Mater.*

Interfaces, vol. 13, no. 50, pp. 59695–59707, Dec. 2021, doi: 10.1021/acsami.1c18740.

37. M. R. F. Muslim, L. Chabib, B. E. Suryaningsih, F. Hayati, and V. Annisa, “Green-synthesized silver nanoparticle hydrogels for biofilm-infected wounds: Bridging sustainability and clinical translation,” *Front. Pharmacol.*, vol. 16, p. 1694144, Oct. 2025, doi: 10.3389/fphar.2025.1694144.
38. W. L. Hasan, R. Sari, and E. Hendradi, “Green Synthesis of Antimicrobial Silver Nanoparticles using Green Tea Extract: The Role of Concentration and pH,” *J Sains Farm Klin*, vol. 11, no. 1, pp. 25–31, Jun. 2024, doi: 10.25077/jsfk.11.1.25-31.2024.
39. L. Torres Neto, M. L. G. Monteiro, B. D. Da Silva, M. A. M. Machado, Y. D. S. Mutz, and C. A. Conte-Junior, “Ultrasound-Assisted Nanoemulsion Loaded with Optimized Antibacterial Essential Oil Blend: A New Approach against Escherichia coli, Staphylococcus aureus, and Salmonella Enteritidis in Trout (Oncorhynchus mykiss) Fillets,” *Foods*, vol. 13, no. 10, p. 1569, May 2024, doi: 10.3390/foods13101569.
40. S. Sharma, A. Bose, S. Biswas, S. Sen, and I. Roy, “Cyperus rotundus mediated green synthesis of silver nanoparticles for antibacterial wound dressing applications,” *Sci Rep*, vol. 15, no. 1, p. 18394, May 2025, doi: 10.1038/s41598-025-03555-x.
41. S. Anju and J. Sarada, “Development and Evaluation of Biogenic Nano-Hydrogel Incorporating Silver Nanoparticles for Wound Healing and Antibiofilm Activity,” *J. Pure Appl. Microbiol.*, vol. 19, no. 3, pp. 1938–1947, Sep. 2025, doi: 10.22207/JPAM.19.3.20.
42. C. Vanlalveni, S. Lallianrawna, A. Biswas, M. Selvaraj, B. Changmai, and S. L. Rokhum, “Green synthesis of silver nanoparticles using plant extracts and their antimicrobial activities: a review of recent literature,” *RSC Adv.*, vol. 11, no. 5, pp. 2804–2837, 2021, doi: 10.1039/D0RA09941D.
43. M. T. Elabbasy *et al.*, “Antibacterial and Antibiofilm Activity of Green-Synthesized Zinc Oxide Nanoparticles Against Multidrug-Resistant Escherichia coli Isolated from Retail Fish,” *Molecules*, vol. 30, no. 4, p. 768, Feb. 2025, doi: 10.3390/molecules30040768.
44. J. A. F. Sutton *et al.*, “Staphylococcus aureus cell wall structure and dynamics during host-pathogen interaction,” *PLoS Pathog*, vol. 17, no. 3, p. e1009468, Mar. 2021, doi: 10.1371/journal.ppat.1009468.

Figures

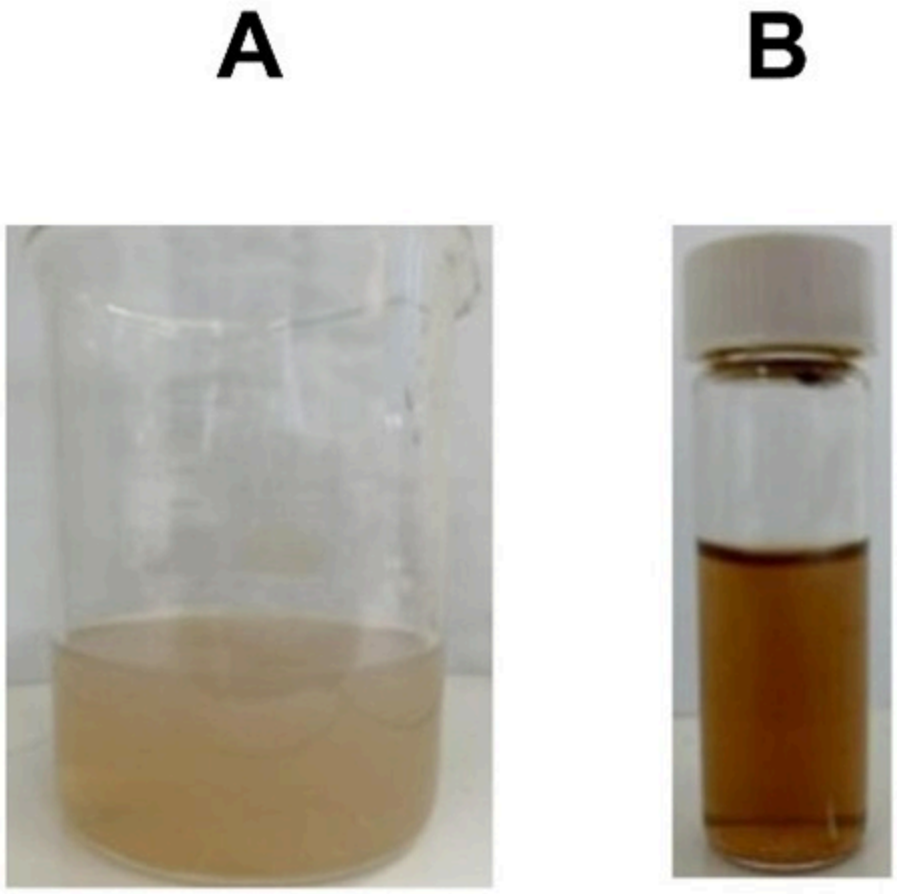

Figure 1

The color observation of biosynthesized AgNPs using Kelakai leaf extract (A) 0 hours, (B) 24 hours.

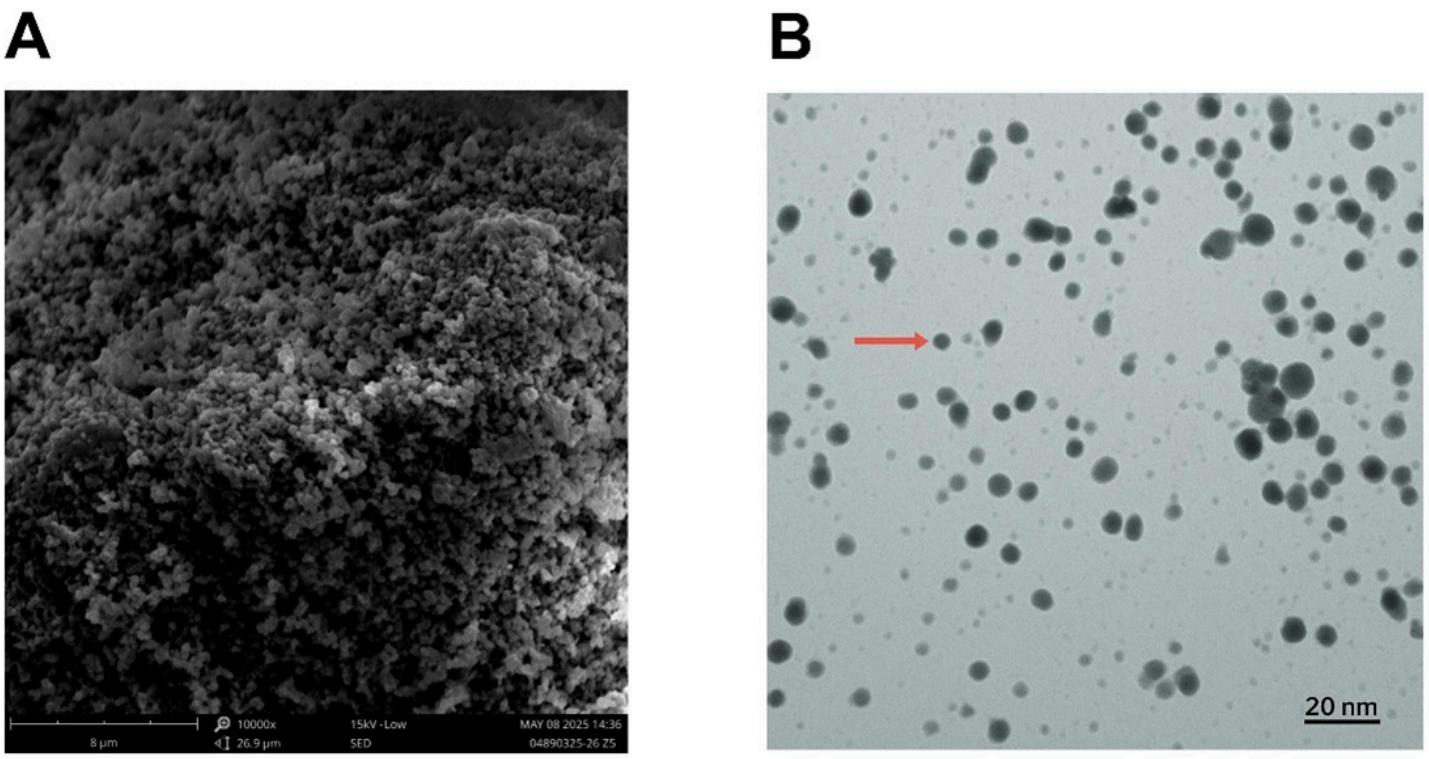

Figure 2

Observation of the morphology of biosynthesized AgNPs using Kelakai leaf extract (a) SEM and (b) TEM

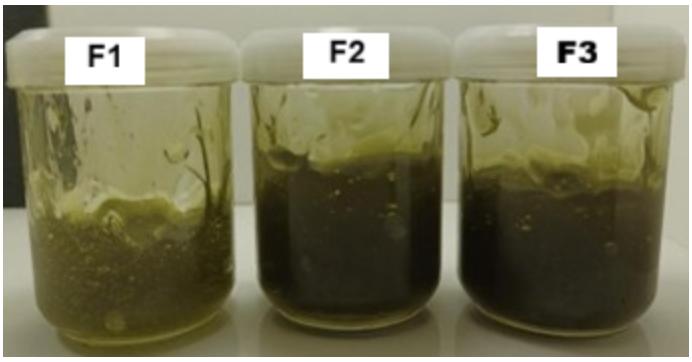

Figure 3

The formulation of biosynthesized AgNPs hydrogel

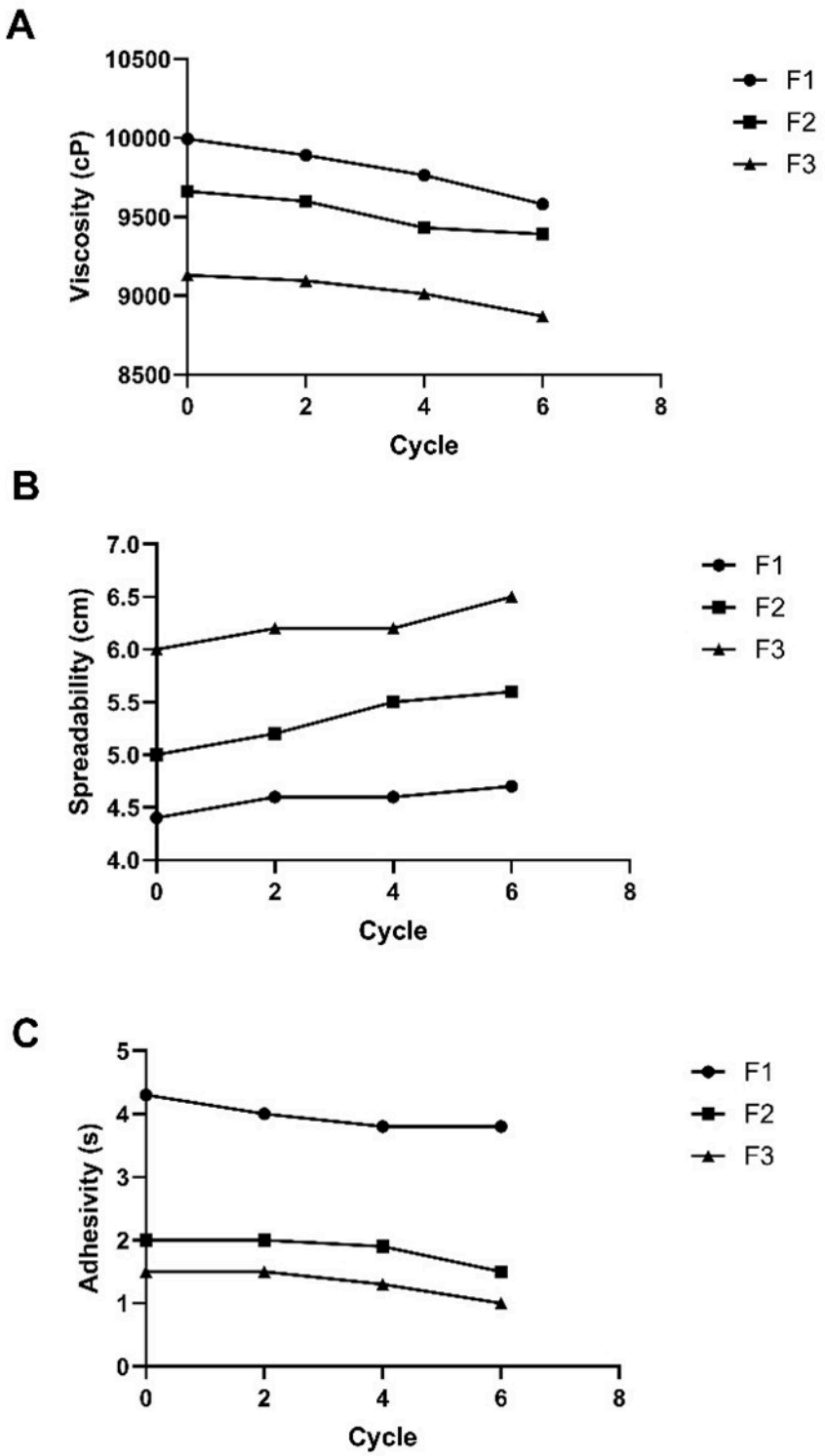

Figure 4

Physical Stability of Formulations (F1–F3) over Six Freeze-Thaw Cycles

(A) Viscosity parameter, (B) Spreadability parameter, and (C) Adhesivity parameter. Each point represents the mean value of measurements.

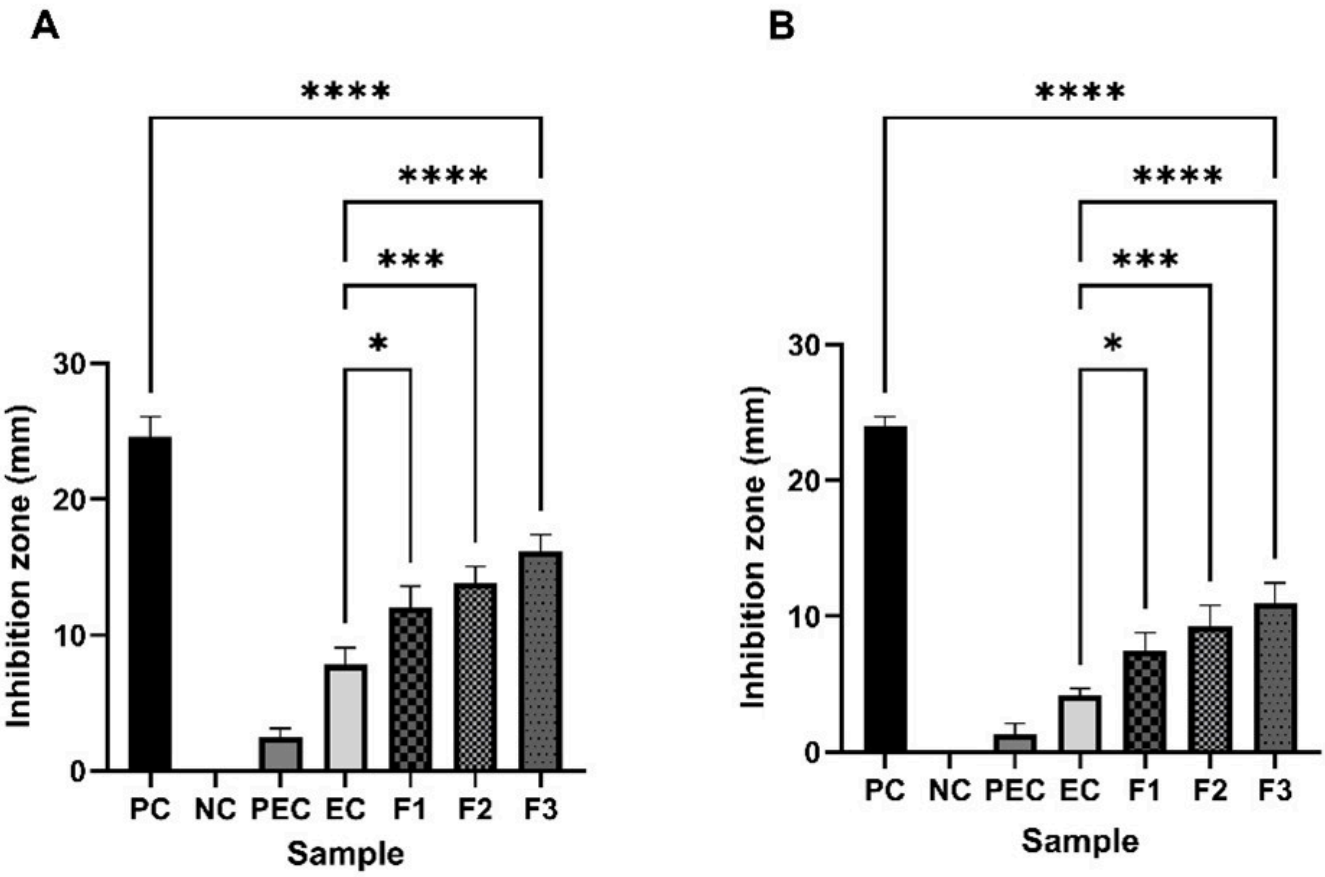

Figure 5

Antibacterial Activity of Formulations against *S. aureus* (A) and *E. coli* (B)

Data represent mean inhibition zones ± S.D. Formulations (F1–F3) showed significantly increased activity compared to extract control (EC). Asterisks indicate statistical significance levels (*: $p < 0.05$, ***: $p < 0.001$, ****: $p < 0.0001$) between treatment groups determined by one-way ANOVA.

PC: Positive control (chloramphenicol), NC: Negative control, PEC: Precursor ($AgNO_3$) control, EC: Extract control, F1: Biosynthesized AgNPs hydrogel Formulation 1, F2: Biosynthesized AgNPs hydrogel Formulation 2, F3: Biosynthesized AgNPs hydrogel Formulation 3

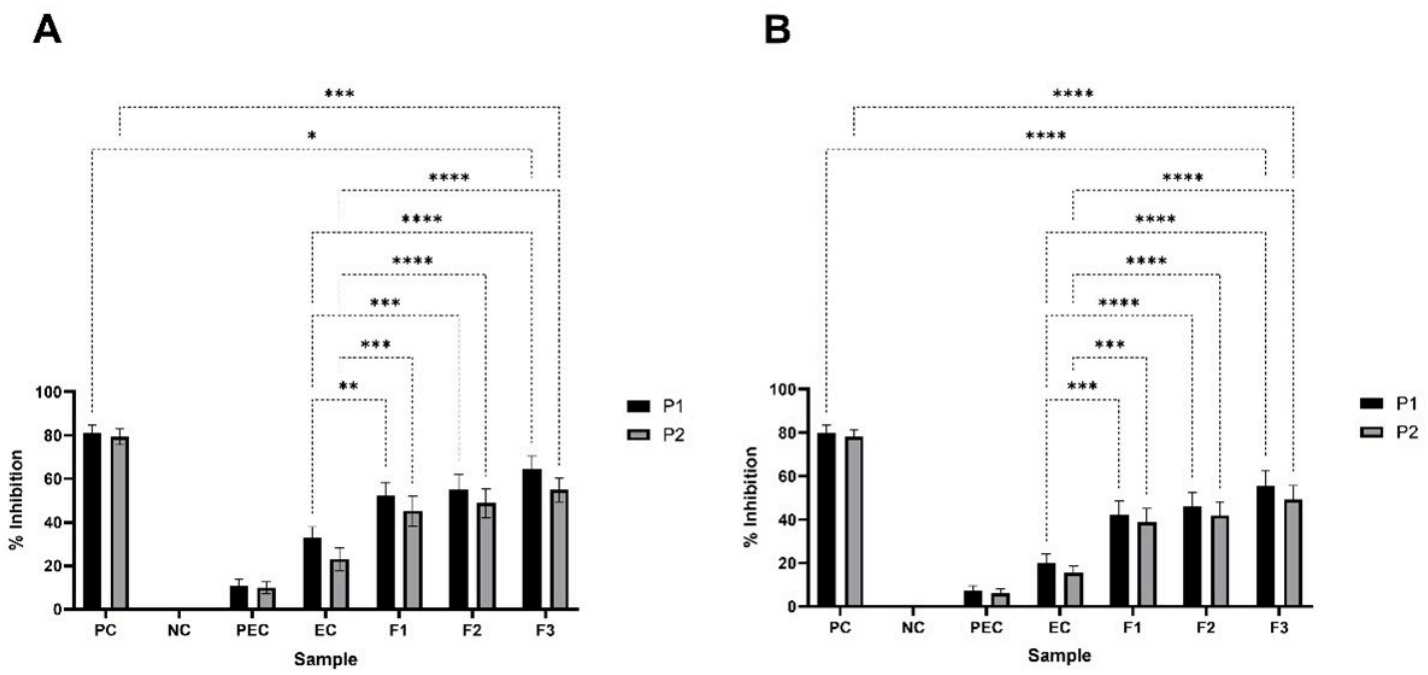

Figure 6

Percentage of Biofilm Inhibition against (A) *S. Aureus*, and (B) *E. coli*

Assays evaluated the prevention of attachment (P1) and the destruction of 24-h formed biofilm (P2). Data represent mean inhibition ± S.D. Formulations (F1–F3) exhibited significantly enhanced antibiofilm activity compared to extract controls (EC), with F3 showing the highest efficacy. Asterisks denote statistical significance levels (*: $p < 0.05$, **: $p < 0.01$, ***: $p < 0.001$, ****: $p < 0.0001$) relative to controls.

PC: Positive control (chloramphenicol), NC: Negative control, PEC: Precursor ($AgNO_3$) control, EC: Extract control, F1: Biosynthesized AgNPs hydrogel Formulation 1, F2: Biosynthesized AgNPs hydrogel Formulation 2, F3: Biosynthesized AgNPs hydrogel Formulation 3

Supplementary Files

This is a list of supplementary files associated with this preprint. Click to download.

- 30032026supportinginformation.docx